Bulletin of Natural Sciences Research
Vol. 15, No. 1, 2025, pp. 78-85.

DOI: https://doi.org/10.5937/bnsr15-59743
Original Scientific Paper

AN INFORMATION-PHYSICAL PERSPECTIVE ON FADING PROCESS TRANSITIONS BASED ON HIGHER ORDER STATISTICS

STEFAN R. PANIĆ[1,⋆]

[1] Faculty of Natural Sciences and Mathematics, University of Priština in Kosovska Mitrovica, Kosovska Mitrovica, Serbia

ABSTRACT

This paper proposes a novel theoretical framework for analyzing fading channels by introducing the concepts of energetic orbits and entropy barriers. Inspired by atomic physics and thermodynamic analogies, here the signal envelope is modeled as a stochastic process whose transitions between different structural regimes (extrema, inflection points, level crossings) correspond to energy quantization events. Each transition is associated with a local information-energy quantum, defined as a product of amplitude displacement and transition count, normalized by local entropy. Furthermore, the ideas of entropic spin and degeneracy of states have been explored, and the dispersion of level-crossing processes, extremum-crossing process, inflection point-crossing process, saddle point-crossing process (LCR, ECR, ICR, SCR) through an autocorrelation-based energetic formalism has been characterized. This approach enables the construction of a layered energetic map of fading dynamics and offers new insights into the structural behavior of wireless signals under stochastic fluctuations.

Keywords: Fading channels, Entropy barriers, Energetic orbits, Crossing statistics, Stochastic signal dynamics.

INTRODUCTION

In modern wireless communications, the fading process represents one of the most critical challenges for maintaining signal integrity and reliability. Fading arises due to the superposition of multiple reflected, refracted, and scattered components of the transmitted signal, leading to time-varying fluctuations in amplitude, phase, and frequency (Simon & Alouini, 2005). These fluctuations can be modeled as stochastic processes with varying statistical properties, depending on environmental and mobility conditions (Stuber, 2001). Classical fading models, such as Rayleigh, Rician, and Nakagami-m, Gamma, Weibull, Hoyt, $\alpha-\mu$, $\kappa-\mu$ and $\eta-\mu$ have been used to characterize signal behavior under different propagation conditions (Panic et al., 2013).

With the advent of 6G and beyond wireless technologies, the demand for ultra-reliable low-latency communication (URLLC), massive machine-type communications (mMTC), and enhanced mobile broadband (eMBB) has led to the need for more refined performance metrics that go beyond traditional outage probability or average bit error rate. In this context, crossing statistics, such as the level crossing rate (LCR) and average fade duration (AFD), have gained prominence as tools to assess the dynamic structure of the fading envelope. These metrics capture how frequently and for how long a signal crosses certain amplitude thresholds, offering a more nuanced understanding of channel behavior in time-sensitive or mission-critical scenarios (Abdi & Nader-Esfahani, 2003).

Building on this perspective, recent theoretical work has extended crossing statistics to include higher-order concepts, such as extremum crossing rate (ECR), inflection point crossing rate (ICR), and saddle crossing rate (SCR). These measures rely on higher-order time derivatives of the fading process and their statistical distributions, enabling a more granular analysis of waveform structure. Despite their potential, a unifying physical or informational interpretation of these metrics remains elusive, especially in connection with signal energetics and system-level implications.

This paper introduces a novel informational-energetic framework that interprets crossing phenomena in fading channels as transitions across entropic barriers and energetic orbital zones. Motivated by analogies to thermodynamic systems, characteristic energy levels associated with crossing statistics has been defined and their interdependence with entropy-like measures and signal variability has been observed. Contribution lies in bridging stochastic signal analysis with conceptual tools inspired by statistical mechanics and information theory, thereby proposing a new lens through which to understand the microstructure of fading dynamics. This framework aims to complement existing analytical methods while offering fertile ground for new interpretations, visualizations, and performance insights in future wireless systems.

SYSTEM MODEL

Let $X(t)$ be a stationary, ergodic random process representing the fading envelope. For a given threshold level u, the LCR quantifies the frequency of signal excursions across level u in both directions, positive and negative crossing (Rice, 1944, 1945):

$$N_u^{(+)} = \int_0^{\infty} \dot{x}\, p_{X,\dot{X}}(u,\dot{x})\, d\dot{x}. \tag{1}$$

and

$$N_u^{(-)} = -\int_{-\infty}^{0} \dot{x}\, p_{X,\dot{X}}(u,\dot{x})\, d\dot{x}. \tag{2}$$

⋆ Corresponding author: stefan.panic@pr.ac.rs

where $p_{X,\dot{X}}(x,\dot{x})$ represents joint probability density function (JPDF) of random process $X(t)$ and its first time derivative $\dot{X}$. The total LCR is in that case then given by:

$$N_u = N_u^{(+)} + N_u^{(-)} = \int_0^{\infty} |\dot{x}|\, p_{X,\dot{X}}(u,\dot{x})\, d\dot{x}. \tag{3}$$

The AFD can be correspondingly derived as (Rice, 1944):

$$\mathrm{AFD}_u = \frac{F_X(u)}{N_u}. \tag{4}$$

where $F_X(u)$ is the cumulative distribution function (CDF) of $X(t)$, while N_u is the total LCR. AFD can be decomposed into upward and downward fade durations as (Tikhonov, 1970):

$$\mathrm{AFD}_u^{(+)} = \frac{F_X(u)}{N_u^{(+)}}, \quad \mathrm{AFD}_u^{(-)} = \frac{F_X(u)}{N_u^{(-)}}. \tag{5}$$

corresponding to upward and downward crossings of level u. Higher-order statistics extend these concepts to the curvature and geometric behavior of the fading process, describing progressively its finer structural properties (Blachman, 1999). ECR quantifies local extrema, ICR captures curvature reversals, and SCR characterizes the sharpness or saddle-like transitions between inflection points. This multiscale statistical perspective is particularly useful in modern communication systems where fine envelope fluctuations directly impact reliability and error dynamics.

As mentioned, ECR counts zero-crossings of $\dot{X}(t)$, capturing local maxima:

$$\eta_u^{\max} = -\int_{-\infty}^{0} \ddot{x}\, p_{X,\dot{X},\ddot{X}}(u,0,\ddot{x})\, d\ddot{x}. \tag{6}$$

and local minima:

$$\eta_u^{\min} = \int_{0}^{\infty} \ddot{x}\, p_{X,\dot{X},\ddot{X}}(u,0,\ddot{x})\, d\ddot{x}. \tag{7}$$

for observed level u of random process. The total ECR is in that case then given by:

$$\eta_u = \eta_u^{\max} + \eta_u^{\min} = \int_{\infty}^{0} |\ddot{x}|\, p_{X,\dot{X},\ddot{X}}(u,0,\ddot{x})\, d\ddot{x}. \tag{8}$$

In similar manner ICR can be observed as characterization related to curvature transitions (changes in concavity). Number of translations from concave to convex process can be obtained as:

$$\kappa_u^{(+)} = \int_0^{\infty} \dddot{x}\, p_{X,\dot{X},\ddot{X},\dddot{X}}(u,\ddot{x},0,\dddot{x})\, d\dddot{x}. \tag{9}$$

while convex-to-concave translations of random procces u can be expressed as:

$$\kappa_u^{(-)} = -\int_{-\infty}^{0} \dddot{x}\, p_{X,\dot{X},\ddot{X},\dddot{X}}(u,\ddot{x},0,\dddot{x})\, d\dddot{x}. \tag{10}$$

The total ICR is in that case then given by:

$$\kappa_u = \kappa_u^{(+)} + \kappa_u^{(-)} = \int_0^{\infty} |\dddot{x}|\, p_{X,\dot{X},\ddot{X},\dddot{X}}(u,\ddot{x},0,\dddot{x})\, d\dddot{x}. \tag{11}$$

The SCR measures the rate at which the third derivative of curvature, $\dddot{X}(t)$, crosses zero, indicating rapid geometric transitions in the signal's shape. It is especially useful in detecting saddle-like behaviors and sharp geometric inflection transitions.

Now let us define SCR as the sum of two directional components: Convex-to-saddle transitions, which can be calculated according to:

$$\chi_u^{(+)} = \int_0^{\infty} x^{(4)}\, p_{X,\dot{X},\ddot{X},\dddot{X},X^{(4)}}(u,\dot{x},\ddot{x},0,x^{(4)})\, dx^{(4)}. \tag{12}$$

and Concave-to-saddle transitions, which can be calculated according to:

$$\chi_u^{(-)} = -\int_{-\infty}^{0} x^{(4)}\, p_{X,\dot{X},\ddot{X},\dddot{X},X^{(4)}}(u,\dot{x},\ddot{x},0,x^{(4)})\, dx^{(4)}. \tag{13}$$

In that case the total CSR is thus expressed as:

$$\chi_u = \chi_u^{(+)} + \chi_u^{(-)} = \int_0^{\infty} |x^{(4)}|\, p_{X,\dot{X},\ddot{X},\dddot{X},X^{(4)}}(u,\dot{x},\ddot{x},0,x^{(4)})\, dx^{(4)}. \tag{14}$$

To extend the concept of AFD to higher-order structural features of the fading process, let us introduce analogous time-domain measures for extrema, inflection points, and saddle geometries, i.e. Average Extrema Duration (AED), Average Inflection Duration (AID) and Average Saddle Duration (ASD). AED metric quantifies the average time between successive extrema (local maxima or minima) below a threshold level u. It is defined as:

$$\mathrm{AED}_u = \frac{P(X<u)}{\eta_u} = \frac{F_X(u)}{\eta_u}. \tag{15}$$

where $F_X(u)$ is the CDF of the fading envelope $X(t)$ and η_u is the total ECR at level u. This metric can be split as:

$$\mathrm{AED}_u^{(\max)} = \frac{F_X(u)}{\eta_u^{\max}}, \quad \mathrm{AED}_u^{(\min)} = \frac{F_X(u)}{\eta_u^{\min}}. \tag{16}$$

to separately quantify the durations between local maxima and local minima.

AID metric measures the average duration between transitions in the curvature of the signal envelope, which correspond to inflection points:

$$\mathrm{AID}_u = \frac{P(X<u)}{\kappa_u} = \frac{F_X(u)}{\kappa_u}. \tag{17}$$

where κ_u is the ICR. Optional directional variants can also be defined:

$$\mathrm{AID}_u^{(+)} = \frac{F_X(u)}{\kappa_u^{(+)}}, \qquad \mathrm{AID}_u^{(-)} = \frac{F_X(u)}{\kappa_u^{(-)}}. \tag{18}$$

For completeness, the same logic can be extended to saddle transitions associated with ASD higher-order derivative crossings:

$$\mathrm{ASD}_u = \frac{F_X(u)}{\chi_u}. \tag{19}$$

where χ_u denotes the SCR, based on zero-crossings of the third derivative of the curvature. It can be decomposed as:

$$\mathrm{ASD}_u^{(\nearrow)} = \frac{F_X(u)}{\chi_u^{(+)}}, \quad \mathrm{ASD}_u^{(\searrow)} = \frac{F_X(u)}{\chi_u^{(-)}}. \tag{20}$$

denoting forward-saddle and backward-saddle transition durations respectively. These generalized duration metrics allow for a multiscale characterization of the temporal structure of the fading process, enabling refined analysis of signal behavior in advanced wireless systems.

In the context of fading processes, the time derivatives of the envelope $X(t)$—such as $\dot{X}(t)$, $\ddot{X}(t)$, and higher orders—are often modeled as zero-mean Gaussian random variables. This assumption is justified for wide-sense stationary and ergodic processes due to the smoothness and symmetry of their autocorrelation structure. Specifically, the variance of the n-th time derivative of $X(t)$, denoted by $\sigma^2_{X^{(n)}}$, is obtained by evaluating the $2n$-th time derivative of the autocorrelation function $R_X(\tau)$ at the origin:

$$\sigma^2_{X^{(n)}} = (-1)^n \left. \frac{d^{2n}}{d\tau^{2n}} R_X(\tau) \right|_{\tau=0}. \tag{21}$$

Assuming zero mean and Gaussianity, the PDF of the n-th time derivative $X^{(n)}$ is:

$$p_{X^{(n)}}(x) = \frac{1}{\sqrt{2\pi\sigma^2_{X^{(n)}}}} \exp\left(-\frac{x^2}{2\sigma^2_{X^{(n)}}}\right). \tag{22}$$

Moreover, for stationary Gaussian processes, time derivatives of even and odd order are uncorrelated and hence statistically independent due to symmetry of the autocorrelation function:

$$\mathbb{E}\left[X^{(n)}(t) \cdot X^{(m)}(t)\right] = 0, \quad \text{for } n+m \text{ odd}.$$

This property simplifies joint PDF formulations used in crossing rate computations involving mixed orders of derivatives.

Let $R_X(\tau)$ denote the ACF of $X(t)$. For isotropic Rayleigh fading:

$$R_X(\tau) = J_0(2\pi f_D \tau). \tag{23}$$

where f_D is the maximum Doppler frequency and $J_0(\cdot)$ is the Bessel function of the first kind. Time derivatives of the process can be computed using:

$$R_{X^{(n)}}(\tau) = \left. \frac{\partial^n}{\partial t^n} \frac{\partial^n}{\partial t'^n} R_X(t - t') \right|_{t=t'}. \tag{24}$$

In example for Rayleigh fading, where the envelope has PDF:

$$p_X(u) = \frac{2u}{\Omega} \exp\left(-\frac{u^2}{\Omega}\right), \quad u \geq 0. \tag{25}$$

the LCR at level u is given by:

$$\nu_u = \sqrt{2\pi} f_D \cdot \frac{u}{\sqrt{\Omega}} \exp\left(-\frac{u^2}{\Omega}\right). \tag{26}$$

where f_D is the maximum Doppler frequency and $\Omega = \mathbb{E}[X^2]$ is the average envelope power. Using the conditional Gaussian approximation, the ECR at level u becomes:

$$\eta_u = 2\sqrt{\frac{6}{\pi}} f_D \cdot \frac{u}{\Omega} \exp\left(-\frac{u^2}{\Omega}\right). \tag{27}$$

where the variances of derivatives are:

$$\sigma^2_{\dot{X}|X} = 2\pi^2 f_D^2 \Omega. \tag{28}$$

$$\sigma^2_{\ddot{X}|X} = 6\pi^4 f_D^4 \Omega. \tag{29}$$

Similarly ICR and SCR values can be determined.

The variance of the number of level crossings $N_u(T)$ during interval $[0, T]$:

$$\mathrm{Var}[N_u(T)] = 2\int_0^T (T - \tau)\left[R_{N_u}(\tau) - N_u^2\right] d\tau. \tag{30}$$

where $R_{N_u}(\tau)$ is the autocorrelation function of the crossing process:

$$R_{N_u}(\tau) = \int_{-\infty}^{\infty}\int_{-\infty}^{\infty} |\dot{x}_1||\dot{x}_2|\, p_{X,\dot{X},X',\dot{X}'}(u, \dot{x}_1, u, \dot{x}_2; \tau)\, d\dot{x}_1\, d\dot{x}_2. \tag{31}$$

The same structure can be used for ECR dispersion:

$$\mathrm{Var}[N_{\dot{X}=0}(T)] = 2\int_0^T (T - \tau)\left[R_\eta(\tau) - \eta^2\right] d\tau. \tag{32}$$

The variance of the number of extremum crossings $N_{\dot{X}=0}(T)$ in the time interval $[0, T]$ is given by:

$$\mathrm{Var}[N_{\dot{X}=0}(T)] = 2\int_0^T (T - \tau)\left[R_\eta(\tau) - \eta^2\right] d\tau. \tag{33}$$

where $R_\eta(\tau)$ is the autocorrelation function of the ECR process, expressed as:

$$R_\eta(\tau) = \int_{-\infty}^{\infty}\int_{-\infty}^{\infty} |\ddot{x}_1||\ddot{x}_2|\, p_{X,\dot{X},\ddot{X},X',\dot{X}',\ddot{X}'}(u, 0, \ddot{x}_1, u, 0, \ddot{x}_2; \tau)\, d\ddot{x}_1\, d\ddot{x}_2. \tag{34}$$

Similarly, the variance of the number of inflection point crossings $N_{\ddot{X}=0}(T)$ over the interval $[0, T]$ is:

$$\mathrm{Var}[N_{\ddot{X}=0}(T)] = 2\int_0^T (T - \tau)\left[R_\kappa(\tau) - \kappa^2\right] d\tau. \tag{35}$$

where the autocorrelation function of the ICR process is given by:

$$R_\kappa(\tau) = \int_{-\infty}^{\infty}\int_{-\infty}^{\infty} d\dddot{x}_1\, d\dddot{x}_2 |\dddot{x}_1||\dddot{x}_2| \\ p_{X,\ddot{X},\dddot{X},X',\ddot{X}',\dddot{X}'}(u, 0, \dddot{x}_1, u, 0, \dddot{x}_2; \tau). \tag{36}$$

Finally, the variance of the number of saddle point crossings $N_{\dddot{X}=0}(T)$ is:

$$\mathrm{Var}[N_{\dddot{X}=0}(T)] = 2\int_0^T (T - \tau)\left[R_\chi(\tau) - \chi^2\right] d\tau. \tag{37}$$

with the ACF of the SCR process:

$$R_\chi(\tau) = \iint_{-\infty}^{\infty} dx_1^{(4)} dx_2^{(4)} |x_1^{(4)}||x_2^{(4)}| \cdot \\ p_{X(t),\ddot{X}(t),\dddot{X}(t),X^{(4)}(t),X(t+\tau),\ddot{X}(t+\tau),\dddot{X}(t+\tau),X^{(4)}(t+\tau)}(u, \ddot{x}_1, 0, x_1^{(4)}, u, \ddot{x}_2, 0, x_2^{(4)}). \tag{38}$$

For each fading model, one can identify characteristic envelope levels at which key stochastic rates attain their maxima. Specifically, the saddle crossing rate (SCR) reaches its maximum

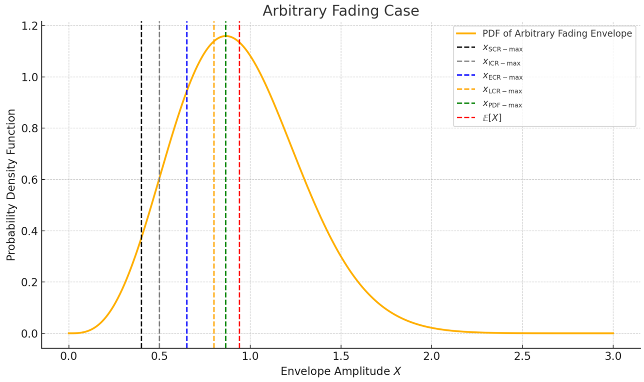

Figure 1. Illustration of the envelope PDF with statistical markers for characteristic crossing metrics.

at the lowest amplitude level, denoted $x_{\mathrm{SCR-max}} = \kappa^{-1}_{u\,\mathrm{max}}(X)$, followed by the inflection crossing rate (ICR) at $x_{\mathrm{ICR-max}}$, the extremum crossing rate (ECR) at $x_{\mathrm{ECR-max}}$, and the level crossing rate (LCR) at $x_{\mathrm{LCR-max}}$. The envelope PDF itself typically peaks at $x_{\mathrm{PDF-max}} = \sigma$, which lies below the statistical mean $\mathbb{E}[X]$. In unimodal and symmetric fading distributions such as Rayleigh or Nakagami-m, this ordering generally holds (see Figure 1):

$$x_{\mathrm{SCR-max}} \leq x_{\mathrm{ICR-max}} \leq x_{\mathrm{ECR-max}} \leq x_{\mathrm{LCR-max}} \leq x_{\mathrm{PDF-max}} \leq \mathbb{E}[X]. \tag{39}$$

This progression reflects a natural gradient from transient and localized features of the envelope (e.g., saddle points) to more stable and probable signal excursions (e.g., mean level crossings).

The entropic envelopes for various crossing-based statistics in fading processes can be formally defined by tracing the loci of their instantaneous local maxima. Each envelope captures a structurally dominant transition zone corresponding to a particular order of derivative behavior in the signal dynamics (Stefanovic et al., 2012).

Let $X(t)$ be a continuous fading process with continuous derivatives up to fourth order. The envelope surfaces corresponding to the maxima of various crossing statistics are defined by:

PDF Envelope:

$$\mathcal{E}_{\mathrm{PDF}} = \arg\max_{x\in\mathbb{R}} \left\{ p_X(x) \;\middle|\; \frac{d}{dx} p_X(x) = 0 \right\}. \tag{40}$$

LCR Envelope:

$$\mathcal{E}_{\mathrm{LCR}}(t) = \arg \max_{\dot{X}(t)=0,\ \ddot{X}(t)<0} X(t). \tag{41}$$

ECR Envelope:

$$\mathcal{E}_{\mathrm{ECR}}(t) = \arg \max_{\dot{X}(t)=0,\ \ddot{X}(t)\neq 0} X(t). \tag{42}$$

ICR Envelope:

$$\mathcal{E}_{\mathrm{ICR}}(t) = \arg \max_{\ddot{X}(t)=0,\ \dddot{X}(t)\neq 0} X(t). \tag{43}$$

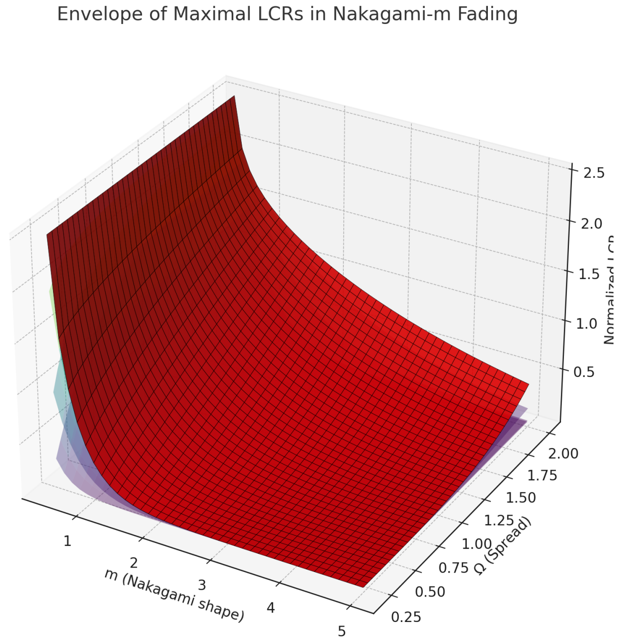

Figure 2. Illustration of the envelope surface of maximums of LCR process of Nakagami-m fading.

SCR Envelope:

$$\mathcal{E}_{\mathrm{SCR}}(t) = \arg \max_{\dddot{X}(t)=0,\ X^{(4)}(t)\neq 0} X(t). \tag{44}$$

These envelopes, individually and collectively, delineate macro-scale statistical boundaries in the signal space and can be interpreted as entropic manifolds — encoding the dominant excursion behavior of the underlying fading process across multiple derivative dimensions. The entropic envelope can be interpreted as a singular solution to a higher-order differential equation that governs the statistical dynamics of the fading process. In this context, the standard statistical measures such as the PDF, LCR, ECR, ICR and SCR represent particular solutions or projections of this governing structure under specific boundary or derivative constraints. While the PDF captures the stationary distribution of the envelope, the derivative-based crossing rates correspond to dynamic transitions across levels of increasing geometric complexity. The envelope thus encodes a global, macro-structural constraint, guiding the formation of localized statistical behaviors and acting as an attractor surface in the space of observable transitions.

Figure 2 illustrates the surface behavior of the normalized LCR in a Nakagami-m fading environment as a function of the fading severity parameter m, the average power Ω, and the signal level u (expressed in decibels). Several semi-transparent LCR surfaces corresponding to fixed values of u are shown to depict the structural variation of the LCR in the 3D parameter space. Overlaid on these surfaces is a prominent red envelope surface that traces the locations of maximum LCR values across all combinations of m and Ω, obtained by solving $\frac{\partial}{\partial u}\mathrm{LCR}(u; m, \Omega) = 0$. This envelope delineates the most probable fluctuation intensities for different fading regimes and serves as a boundary surface separating regions of deterministic behavior from those dominated by stochastic excursions, supporting the concept of entropic zones in fading dynamics.

RESULTS AND DISCUSSION

Entropic Envelopes and Structural Boundaries of Fading Processes

The concept of *entropic envelopes* is proposed as a statistical framework to characterize the structural transitions within stochastic fading processes. These envelopes are defined as boundary surfaces composed of local maxima of key statistical rate functions, namely: PDF, LCR, ECR, ICR, SCR. Each of these rate functions encodes a distinct type of structural behavior of the fading envelope.

- The first boundary, denoted $x^{\max}_{\mathrm{PDF}}$, corresponds to the most probable signal level, i.e., the maximum of the PDF. This point represents the mode of the process and serves as a statistical center of mass for the fading distribution.
- The LCR envelope corresponds to amplitude-level crossings (zero-crossings of the first derivative). Its maximum, $x^{\max}_{\mathrm{LCR}}$, identifies the most likely signal level where crossings of a fixed threshold occur.
- The ECR envelope tracks local maxima and minima by identifying points where the first derivative vanishes and the second derivative is non-zero. The maximum $x^{\max}_{\mathrm{ECR}}$ denotes the dominant structural oscillation scale.
- The ICR envelope captures inflection points (zero-crossings of the second derivative with non-zero third derivative). $x^{\max}_{\mathrm{ICR}}$ marks transitions in curvature and delineates regions of acceleration in signal fluctuation.
- The SCR envelope reflects higher-order geometric transitions by locating points where the third derivative vanishes and the fourth derivative is non-zero. The maximum $x^{\max}_{\mathrm{SCR}}$ defines saddle-like changes in the envelope's trajectory, representing the outermost boundary of structured variation.

The positions of these maxima, ordered as:

$$x^{\max}_{\mathrm{SCR}} \le x^{\max}_{\mathrm{ICR}} \le x^{\max}_{\mathrm{ECR}} \le x^{\max}_{\mathrm{LCR}} \le x^{\max}_{\mathrm{PDF}}.$$

serve to partition the signal domain into hierarchical *entropic zones*, where each successive zone represents an increased level of local irregularity or complexity in the signal structure.

Physically, these envelopes can be interpreted as phase-like statistical boundaries that separate regions of predictable, smooth envelope behavior from those dominated by rapid transitions and complexity. In this sense, they form a spectrum of stochastic regularity, useful for defining operational regimes in wireless communication systems. From a practical standpoint, entropic envelopes support tasks such as adaptive modulation, outage prediction, and time-frequency signal classification by providing natural demarcations in the dynamics of the fading process.

Orbital Interpretation of Transitions

Each zone defined by the maxima of LCR, ECR, ICR, and SCR can be conceptualized as an orbital level, similar to discrete energy states in quantum mechanical systems. In that way it can be observed that structural patterns in the fading envelope tend to cluster within well-defined entropic zones. The transitions between these zones represent quantum energy-like changes in the statistical configuration of the process.

From this perspective, a crossing from a local minimum to a maximum, or from an extremum to an inflection point, can be seen as a statistical excitation or relaxation. The system exhibits quantized patterns of movement between these zones, governed by the underlying autocorrelation structure and derivative variances.

This analogy provides a powerful framework to analyze the spectral behavior of fading processes. It allows us to assign structural transitions to distinct entropic orbitals, each characterized by a dominant derivative feature and its associated variance. This interpretation supports the development of quantized information models for wireless fading dynamics.

Directional Characterization of Structural Transitions

To provide a finer classification of the structural transitions in the fading envelope, a directional labeling scheme that characterizes the polarity and orientation of each transition event can be introduced. Specifically, transitions are categorized based on whether they represent an ascent (e.g., from an inflection point to a local maximum) or a descent (e.g., from a maximum to a subsequent inflection or minimum). This directionality reflects the temporal asymmetry in the envelope's evolution.

Incorporating this directional information enriches the structural taxonomy associated with the entropic envelope framework. Each entropic zone, defined by features such as maxima, inflections, or saddle points, can now be associated not only with its morphological type but also with the directional trajectory that the envelope follows through it. This dual classification captures both the geometric structure and the dynamical flow of the signal process.

Such directional analysis becomes particularly valuable in environments exhibiting asymmetry or spatial non-stationarity, such as in multi-antenna or frequency-selective fading scenarios. By distinguishing ascending from descending transition paths, this framework enhances the ability to identify transient versus stable phenomena in the signal, improving both analytical insight and predictive capability in practical systems.

Let $X(t)$ be a continuous envelope process defined on the interval $t \in [0, T]$, and let $X^{(n)}(t)$ denote its n-th time derivative. For any structural transition of order n, we define the directional counts:

$$N^{(n)}_{+}(T) = \#\left\{t_i \in [0, T] \;\middle|\; X^{(n)}(t_i) = 0,\ X^{(n+1)}(t_i) < 0\right\}. \tag{45}$$

$$N^{(n)}_{-}(T) = \#\left\{t_i \in [0, T] \;\middle|\; X^{(n)}(t_i) = 0,\ X^{(n+1)}(t_i) > 0\right\}. \tag{46}$$

The total number of directional transitions of order n is then given by:

$$N^{(n)}(T) = N_+^{(n)}(T) + N_-^{(n)}(T). \tag{47}$$

As a concrete example, for the second-order transitions corresponding to local extrema (ECR events), we have:

$$N_+^{(2)}(T) = \#\left\{t_i \in [0, T] \;\middle|\; \dot{X}(t_i) = 0,\ \ddot{X}(t_i) < 0\right\}, \quad \text{(maxima)}. \tag{48}$$

$$N_-^{(2)}(T) = \#\left\{t_i \in [0, T] \;\middle|\; \dot{X}(t_i) = 0,\ \ddot{X}(t_i) > 0\right\}, \quad \text{(minima)}. \tag{49}$$

This framework thus generalizes to any transition order n, and enables a rigorous classification of the signal's structural dynamics by associating both morphological and directional information with each observed transition.

To quantify the informational complexity of directional transitions, we define an entropy-based metric over the normalized counts of upward and downward events. Let:

$$p_+^{(n)} = \frac{N_+^{(n)}(T)}{N^{(n)}(T)}, \qquad p_-^{(n)} = \frac{N_-^{(n)}(T)}{N^{(n)}(T)}. \tag{50}$$

with $p_+^{(n)} + p_-^{(n)} = 1$. The directional transition entropy is then given by:

$$H_n = -p_+^{(n)} \log_2 p_+^{(n)} - p_-^{(n)} \log_2 p_-^{(n)}. \tag{51}$$

This entropy attains its maximum value $H_n = 1$ when both transition types are equally likely, indicating maximal uncertainty in directionality. Lower values reflect an asymmetry or bias in transition polarity, which may correspond to a directional drift or non-stationarity in the envelope dynamics.

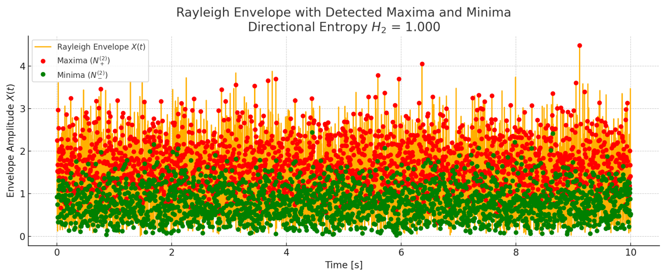

Figure 3. Rayleigh fading envelope with identified local extrema over time.

Red dots at Fig. 3 indicate upward second-order transitions (local maxima), while green dots mark downward second-order transitions (local minima). The underlying signal $X(t)$ is shown in orange. The balance between the number of maxima $N_+^{(2)}$ and minima $N_-^{(2)}$ yields a directional entropy of $H_2 = 1.000$, indicating complete symmetry in the polarity of second-order transitions. This statistical symmetry reflects the ergodicity and isotropy of the Rayleigh fading model and supports the assumption of equal probability for structural ascent and descent events.

Assuming the process $X(t)$ is ergodic and wide-sense stationary over a finite observation window of duration T, the average waiting time between directional transitions of order n can be expressed as:

$$\mathbb{E}[\Delta t_+^{(n)}] = \frac{T}{N_+^{(n)}(T)}. \tag{52}$$

$$\mathbb{E}[\Delta t_-^{(n)}] = \frac{T}{N_-^{(n)}(T)}. \tag{53}$$

where $N_+^{(n)}(T)$ and $N_-^{(n)}(T)$ denote the total number of ascending and descending transitions of the n-th order observed within the interval $[0, T]$. The time horizon T represents the total observation period over which the statistical averages are estimated.
These quantities provide temporal scales over which structural transitions of a given direction and order typically occur. For example, a lower $\mathbb{E}[\Delta t_+^{(2)}]$ implies frequent upward extrema (local maxima), possibly indicating bursty or rapidly varying behavior in the envelope. The full set $\{\mathbb{E}[\Delta t_\pm^{(n)}]\}$ across several n-values can be interpreted as a *temporal fingerprint* of the stochastic structure, with potential applications in classification, anomaly detection, and adaptive system design.

Finally, an entropy-weighted transition index for order n can be defined as:

$$Q^{(n)} = \frac{H_n}{\mathbb{E}[\Delta t^{(n)}]}. \tag{54}$$

where $\mathbb{E}[\Delta t^{(n)}] = T/N^{(n)}(T)$ is the average inter-event duration for all transitions of order n. This metric reflects the *informational flux density* of structural transitions, combining their rate and directional uncertainty. High values of $Q^{(n)}$ indicate both frequent and directionally unpredictable transitions, while lower values point to either sparsity or determinism in the process dynamics.

Entropic-Informational Structure of Derivative Transitions

The entropic-informational structure of a stochastic envelope process is characterized through a hierarchy of statistical transition functions, each associated with a specific time-derivative order of the underlying ACF. These functions namely the LCR, ECR, ICR, SCR, capture the envelope's structural complexity at increasing levels of geometric differentiation.

Each crossing function highlights localized regions of elevated statistical activity, where the envelope exhibits critical morphological features such as amplitude crossings, extrema, curvature sign changes, or higher-order saddle points. These transitions are intrinsically tied to the variances of the corresponding derivatives of the process and reflect the concentration of structural dynamics in specific signal regions.

By systematically analyzing these features, one obtains a compact representation of the envelope's geometric irregularities and their distribution across scales. This derivative-based characterization facilitates rigorous classification of stochastic signals in terms of entropic density and structural coherence, offering valuable insights for tasks such as fading channel modeling, signal classification, and adaptive information encoding in complex wireless environments.

Transition Quanta and Characteristic Energies

Each transition between entropic zones can be quantified using an informational-energy expression, defining the transition quantum as:

$$q_i = \frac{\Delta u_i \cdot \Delta N_i}{p_i \log(p_i)}. \tag{55}$$

where Δu_i is the level excursion, ΔN_i is the number of transitions in that zone, and p_i is the transition probability. The total information quantum can be in that case computed as the inverse harmonic sum:

$$Q^{-1} = \left(\sum_i \frac{1}{q_i}\right)^{-1}. \tag{56}$$

The characteristic energy of the nth-order transition zone is defined through the autocorrelation of the corresponding crossing process:

$$2T\int_0^T (T-\tau)[R_{N^{(n)}}(\tau) - (\nu_u^{(n)})^2]d\tau = H(X^{(n)}) \cdot Q^{-1}. \tag{57}$$

where $H(X^{(n)})$ is the entropy of the nth derivative of the process.

The entropy can be given by:

$$H(X^{(n)}) = \frac{1}{2} + \frac{1}{2}\log(2\pi\sigma^2_{X^{(n)}}). \tag{58}$$

This framework connects transition rates with both informational content and energy expenditure, providing a dual view of envelope complexity.

Structural transitions in fading processes may converge when higher-order features of the envelope become indistinct. Specifically, critical points such as local maxima may gradually lose curvature and merge with neighboring inflection points, thereby collapsing distinct entropic zones into a unified region of statistical indeterminacy. This transition signifies the onset of what can be termed an *entropic continuum*, where discrete morphological events become indistinguishable.

Within this continuum regime, the envelope process exhibits increased stochastic irregularity, characterized by an absence of clear-cut extrema, inflection points, or saddle structures. The geometric regularity of the signal deteriorates, and the fading process approaches a structurally chaotic behavior. Under these conditions, classical descriptors fail to isolate features, and one must instead rely on global metrics such as crossing densities, spectral entropy, or cumulant-based statistics to quantify complexity.

The total number of structural excursions accumulated across all entropic orders provides a macroscopic measure of this complexity:

$$N_{\text{total}} = \sum_i N^{(i)}. \tag{59}$$

where $N^{(i)}$ represents the number of transitions of structural order i. This aggregate count offers a coarse-grained but comprehensive summary of the signal's morphological dynamics.

Entropic Potential and Informational Transition Fields

To characterize the directional bias and local dynamics of structural evolution in fading processes, we introduce the notion of an *entropic potential field*. This scalar function encapsulates the tendency of the signal envelope to transition through distinct morphological states, driven not by classical energy considerations, but by local informational gradients.

Let $\mathcal{U}(x)$ denote the entropic potential at envelope level x. One possible formalization connects $\mathcal{U}(x)$ to the derivative of the autocorrelation function $R_X^{(n)}(\tau)$, or to the derivative of the crossing density function. An alternative formulation ties it to the normalized transition quantum q_i via Eq.55, where Δu_i and ΔN_i denote amplitude and transition count variations within zone i, and p_i is the normalized probability of such transitions. These local information-energy interactions define the entropic geometry of the process.

The entropic potential field defines an informational gradient landscape that directs the evolution of the stochastic envelope between regions of relative stability and instability. Analogous to physical systems, this potential may exhibit local minima, interpreted as informational attractors and local maxima, corresponding to repelling configurations. These structural extrema delineate statistically dominant regimes within the signal space. This framework provides a rigorous basis for enhancing signal processing strategies in adaptive wireless systems, including channel state estimation, predictive modeling, and rate adaptation under non-stationary fading conditions.

Entropic Potential Function for Structural Transitions

For a generic structural transition of order n, the entropic potential function $\mathcal{U}^{(n)}(x)$ can be defined as:

$$\mathcal{U}^{(n)}(x) = -\log\left(\frac{N^{(n)}(x)}{\max_x N^{(n)}(x)}\right). \tag{60}$$

where:

- $N^{(n)}(x)$ is the crossing rate function of order n (e.g., LCR for $n = 1$, ECR for $n = 2$, etc.),
- $\max_x N^{(n)}(x)$ is the global maximum of the crossing rate function over the signal domain x,

Interpretation:

- Low potential values $\mathcal{U}^{(n)}(x) \approx 0$ indicate high likelihood of structural transitions, forming informational *wells*.
- High potential values reflect statistically rare transitions, forming entropic *barriers*.
- The potential profile $\mathcal{U}^{(n)}(x)$ reveals the spatial concentration of structural events and helps delineate the stochastic geometry of the envelope process.

These curves presented at Fig. 4 highlight the *informational landscape* of the signal, where valleys indicate statistically dominant transitions (most likely signal levels), and peaks represent entropic barriers or rare events.

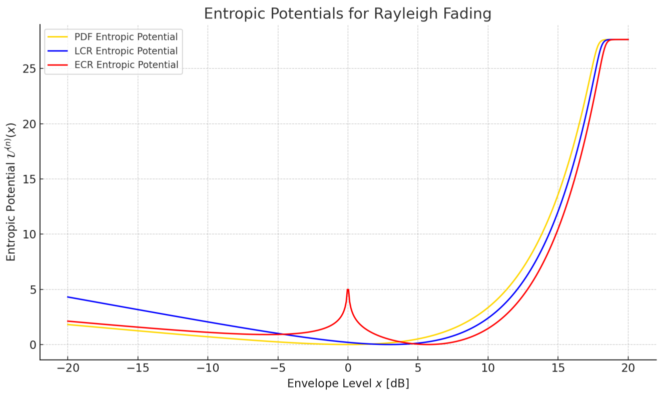

Figure 4. Entropic potentials for Rayleigh fading.

Energy-Entropy Transformation

Two fundamental transformation directions in the study of entropic zones can be identified. The first, energy-to-entropy, observes how structural events such as maxima and saddles can be mapped to entropic zones via their statistical significance. This results in an entropic spectrum that characterizes the process's disorder. The second transformation, entropy-to-energy, aggregates the local information contributions (via $H(X^{(n)})$) across derivative orders to reconstruct energy-like measures. This enables the synthesis of predictive models that treat entropy as a form of latent structural energy. Together, these dual transformations establish a bridge between physical interpretation and information-theoretic representation of stochastic fading envelopes. They offer a unified framework for analyzing complexity and transitions in dynamic systems.

Practical Applications of Study

The entropic envelopes derived from LCR, ECR, ICR, and SCR maxima delineate statistically significant signal regimes, which can inform adaptive modulation and coding strategies. For example, regions corresponding to low entropic potential indicate high transition density and increased signal variability, suggesting the need for robust coding schemes or fallback modulation orders. Conversely, zones with reduced structural activity allow for more aggressive spectral efficiency. Moreover, the entropy-weighted transition index $Q^{(n)}$ and directional entropy H_n provide powerful tools for anomaly detection. Abrupt changes in these metrics over time may signal deviations from normal fading behavior due to interference, obstruction, or hardware faults. In multi-antenna and cooperative systems, the identification of directional asymmetry through $N_{\pm}^{(n)}$ enables intelligent diversity combining by prioritizing channels that exhibit more favorable structural stability. Collectively, these descriptors form a compact statistical signature of the fading environment that can be exploited for real-time adaptation and resilience in dynamic wireless channels.

CONCLUSION

In this work, we introduced a novel framework for the structural analysis of stochastic fading processes through the concept of *entropic envelopes*, which identify and classify the most statistically significant transitions within the signal envelope. By systematically analyzing the local maxima of the LCR, ECR, ICR, SCR, corresponding envelope surfaces are constructed that represent the statistical basis for the fading dynamics. These surfaces highlight regions of high transition density and define operational boundaries within the signal space. Building upon these crossing based features, a directional transition taxonomy based on the sign of higher-order derivatives have been proposed, with introducing quantities such as $N_{+}^{(n)}$, $N_{-}^{(n)}$, and associated waiting times. This helped to define an entropy based index H_n that quantifies the balance of structural transitions, and a derived entropic flux density $Q^{(n)}$, which jointly measures the frequency and unpredictability of such events. Together, these descriptors offer a compact temporal fingerprint of the stochastic envelope process. Furthermore, the notion of an *entropic potential* $U^{(n)}(x)$ has been introduced, analogous to potential energy landscapes, capturing the informational cost of observing a transition at a given signal level x. Finally, an analogy with quantum orbitals was discussed, where structural transitions occupy discrete entropic zones, and degeneracy leads to the merging of these zones into an entropic continuum. This perspective opens new pathways for the quantized modeling of fading dynamics and their application in statistical signal processing and wireless communication system design.

REFERENCES

Abdi, A. & Nader-Esfahani, S. 2003, Expected number of maxima in the envelope of a spherically invariant random process, IEEE Transactions on Information Theory, 49 (6), pp. 1560–1570.

Blachman, N. M. 1999, The distributions of local extrema of Gaussian noise and of its envelope, IEEE Transactions on Information Theory, 45 (7), pp. 2115–2121.

Panic, S., Stefanović, M., Anastasov, J., & Spalević, P. 2013, Fading and interference mitigation in wireless communications (Boca Raton, FL, USA: CRC Press)

Rice, S. O. 1944, Mathematical analysis of random noise, Bell System Technical Journal, 23 (3), pp. 282–332.

Rice, S. O. 1945, Mathematical analysis of random noise—Part II, Bell System Technical Journal, 24 (1), pp. 46–156.

Simon, M. K. & Alouini, M. S. 2005, Digital communication over fading channels, 2nd edn. (Hoboken, NJ, USA: Wiley)

Stefanovic, H., Stefanovic, I., Milic, D., & Stefanovic, D. 2012, in Proceedings of the 11th International Symposium INFOTEH-JAHORINA (Jahorina, Bosnia and Herzegovina: University of East Sarajevo), pp. 1–4.

Stuber, G. L. 2001, Principles of mobile communication, 2nd edn. (Boston, MA, USA: Kluwer Academic)

Tikhonov, V. I. 1970, Excursions in random processes (Moscow, Russia: Nauka), (in Russian)